

## Photochemical Reactions of Actinide Ions

Hiroshi TOMIYASU

Research Laboratory for Nuclear Reactors  
Tokyo Institute of Technology  
O-okayama, Meguro-ku, Tokyo 152, Japan

This paper reviews the results of photochemical studies of actinide ions, which have been performed in our research group for past several years as follows: I) behavior of the excited uranyl(VI) ion<sup>1-6</sup>; II) photo-reductions of the uranyl ion with organic and inorganic compounds<sup>7-10</sup>; III) photo-oxidations of uranium(IV) and plutonium(III) in nitric acid solutions<sup>11-13</sup>.

Keyword: Photochemistry, Uranium, Reaction, Laser, NMR

### I INTRODUCTION

Extensive studies have been reported on the photochemistry of uranyl ions for mainly basic photochemical interest. However, recently interest has been focused on the photochemical method of adjusting the valencies of actinide ions in the nuclear fuel reprocessing. This paper presents the results of photochemistry of actinide ions, mainly uranyl ion, in order to gain better understanding for the practical purpose.

#### I I Behavior of Excited Uranyl Ion

##### *Deactivation Mechanism of the Excited Uranyl Ion*

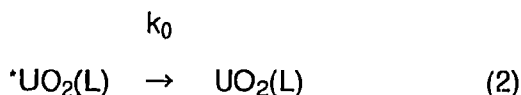
Despite extensive studies on the life-times of the excited uranyl ion and its quenching rate constants, the quenching mechanism of the excited uranyl was much confused for a past decade. This might owe mainly to the dual luminescence of the uranyl ion as described below:

$$I = I_{01}\exp(-k_1t) + I_{02}\exp(-k_2t) \quad (1)$$

where  $I_{01}$  and  $I_{02}$  refer to luminescence intensities at time = 0, and  $k_1$  and  $k_2$  are the

decay constants. We concluded that the dual luminescence was attributed to the emission from independent two species, the excited aqua ion  $^*UO_2^{2+}$  and excited hydrolyzed species  $^*(UO_2)_2(OH)_2^{2+}$  by the following reason. It was found in our studies that the  $^{17}O$  resonance of uranyl oxygen atoms, which was a single Lorentzian curve in strongly acidic solutions, revealed two distinct peaks at  $pH > 3$ . These two peaks were assigned to  $UO_2^{2+}$  and  $(UO_2)_2(OH)_2^{2+}$  (expressed as (2,2) hereafter), and the rate constant for the exchange between these species were determined to be 59.3 and 93.8  $s^{-1}$  at a  $pH$  3.15 for the forward and reverse processes, respectively. Since the above exchange is much slower than the luminescence decay, the species  $^*UO_2^{2+}$  and  $^*(2,2)$  were considered to exist independently within the time scale of uranyl luminescence. The emission from  $^*UO_2^{2+}$  and  $^*(2,2)$  were observed in time resolved emission spectra, where the spectrum at earlier 0.2  $\mu s$  corresponded to the emission of  $^*UO_2^{2+}$ , while the final spectrum at 9.2  $\mu s$  to that of  $^*(2,2)$ .

The quenching of uranyl luminescence is of particular interest and many studies have been performed. For a deeper understanding of quenching reactions, we measured quenching rate constants for various complexes,  $UO_2^{2+}$ ,  $(UO_2)_2(OH)_2^{2+}$ ,  $UO_2(H_2PO_4)_2$  and  $UO_2F_4^{2-}$ , in the presence ( $k_q$ ) and absence ( $k_0$ ) of halogen and halogen-like anions. Figure 1 represents plots of  $\log k_q$  versus  $\log k_0$ . In Fig. 1, the plots are linear for each quencher and all lines join at one point. This is explained well in terms of a linear free-energy relationship. In the absence of quenchers, the decay of excited uranyl complexes  $^*UO_2(L)$ , where L denotes a ligand such as  $H_2O$  or  $F^-$ , can be described by



The linear free-energy relationship leads to the equation:

$$\Delta G_0^*(L) = \Delta G_E^* + a\Delta G(L) \quad (3)$$

Where  $\Delta G_0^*(L)$  is the free energy of activation of reaction (2),  $\Delta G_E^*$  is the free energy of activation for an excited complex,  $^*UO_2(E)$ , which is in the hypothetically highest energy state,  $\Delta G(L)$  is the difference of free energies between  $^*UO_2(L)$  and  $^*UO_2(E)$ , and  $a$  is a constant. In solutions containing quenching anions  $X^-$ , the reaction can be expressed by



leading to the equation:

$$\Delta G_q^*(L) = \Delta G_q^* + b_x \Delta G(L) \quad (5)$$

where  $\Delta G_q^*(L)$  is the free energy of activation of reaction (5),  $\Delta G_q^*$  the free energy of activation for the quenching reaction of  ${}^*UO_2(E)$  and  $b_x$  refers to a constant, which differs as a function of quenchers. Elimination of  $\Delta G(L)$  from (3) and (5) gives the following equation

$$\Delta G_q^*(L) = (b_x/a) \Delta G_0^*(L) + \text{constant} \quad (6)$$

$$\text{constant} = \Delta G_q^* - (b_x/a) \Delta G_E^*$$

Equation (6) is consistent with

$$\ln k_q = (b_x/a) \ln k_0 + \text{constant} \quad (7)$$

which is demonstrated in Fig. 1. The point in this figure where all the lines cross (we call this point as an isoquenching point) gives the maximum decay constant, which might be attributed to the decay of  ${}^*UO_2(E)$ , where  $a = b = 0$ , and  $\Delta G_0^*$  and  $\Delta G_q^*$  would have minimum values.

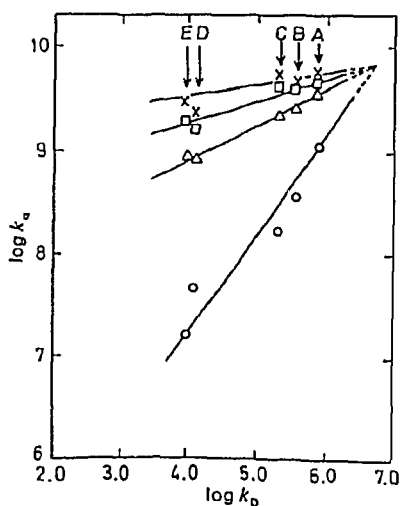


Fig. 1 Plots of  $\log k_q$  versus uranyl complexes.  $k_q$  was determined for the following quenchers: (x)  $I^-$ , ( $\square$ )  $SCN^-$ , ( $\Delta$ )  $Br^-$ , (O)  $Cl^-$ . A,  $UO_2^{2+}$ ; B,  $UO_2SO_4$ ; C,  $(UO_2)_2(OH)_2^{2+}$ ; D,  $UO_2(H_2PO_4)_2$ ; E,  $UO_3F_2^-$ .

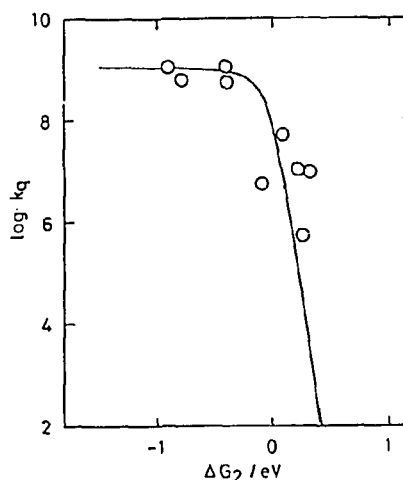


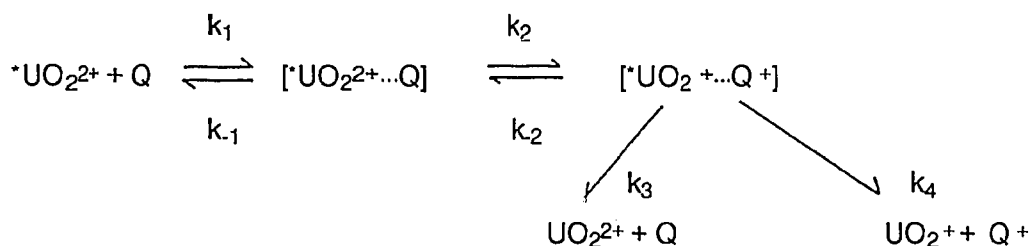
Fig. 2 Plot of  $\log k_q$  vs.  $\Delta G_2$ ;  $k_1 = 1.5 \times 10^9 \text{ mol}^{-1} \text{ dm}^3 \text{ s}^{-1}$ ,  $k_{-1}/Z = 0.25$  and  $\Delta G_2^*(0) = 10.1 \text{ kJ mol}^{-1}$ .

### Quenching of the Excited Uranyl Ion by N-heteroaromatic Compounds

The quenching of the excited uranyl ion by N-heteroaromatic compounds appear to be most interesting among similar quenching reactions of the excited uranyl ion by organic compounds. Quenching rate constants  $k_q$  of uranyl emission were determined in aqueous solutions by measurements of lifetime of the excited uranyl ion by using the following equation

$$k = k_0 + k_q[Q] \quad (1)$$

where  $k$  and  $k_0$  refer to the decay constants of the excited uranyl ion in the presence and absence quenchers, respectively and  $[Q]$  is the concentration of N-heteroaromatic compound. It was found that  $k_q$  decreased with the increasing vertical ionization potential  $I_p$ . This suggests that the quenching of  ${}^*UO_2^{2+}$  proceeds via an electron transfer mechanism with the quenchers. In order to explain the electron transfer mechanism, it is reasonable to presume that  ${}^*UO_2^{2+}$  interacts with N-heteroaromatic compound  $Q$  to form an exciplex or encounter complex  $[{}^*UO_2^{2+}\cdots Q]$ , because of the  $\pi$ -bonding ability of the N-heteroaromatic compounds. Then the exciplex undergoes intramolecular electron transfer to form an unstable intermediate  $[{}^*UO_2^+ \cdots Q^+]$ , which further undergoes reverse electron transfer to form  $UO_2^{2+}$  and  $Q$  or simply decomposes to  $UO_2^+$  and  $Q^+$ . On the basis of the above electron transfer mechanism, the quenching reaction can be written as a sequence of elementary steps as follows:



The steady state approximation leads to eq. (2) for the quenching rate constant  $k_q$ .

$$k_q = k_1 / \{1 + (k_{-1}/k_2)\} \{1 + k_{-2}/(k_3/k_4)\} \quad (2)$$

Since no photochemical products of  $UO_2^{2+}$ , such as  $UO_2^+$  or  $U(IV)$ , were observed on prolonged irradiation of the solutions containing  $UO_2^{2+}$  and the quenchers, the  $k_3$  path is expected to be much faster than the  $k_4$  path, i.e.,  $k_3 \gg k_4$ . On this basis, eq. 2 can be transformed into eq. (3) with  $k_3 \sim Z$

$$k_q = k_1 / \{1 + (k_{-1}/Z)\} \{ \exp(\Delta G_2^*/RT) + \exp(\Delta G_2/RT) \} \quad (3)$$

where  $\Delta G_2$  is the free energy change involved in the electron transfer process from quencher to excited uranyl ion,  $\Delta G_2^*$  is the activation free energy for the  $k_2$  path and  $Z$  is the frequency factor. The value of  $\Delta G_2$  were estimated from the following equation derived from Rehm and Weller

$$\Delta G_2 = E(Q/Q^+) - E(UO_2^+/UO_2^{2+}) - \Delta E_{0,0}(^*UO_2^{2+}) - e_0^2 / \epsilon a \quad (4)$$

where  $E(Q/Q^+)$  and  $E(UO_2^+/UO_2^{2+})$  are the redox potentials of quenchers and uranyl ion respectively,  $\Delta E_{0,0}(^*UO_2^{2+})$  is the energy of the excited uranyl ion and  $e_0^2 / \epsilon a$  is a term which takes into account the solvent properties for ion separation.

$\Delta G_2^*$  can be calculated by the Rehm-Weller empirical equation

$$\Delta G_2^* = \Delta G_2/2 + \{(\Delta G_2/2)^2 + \Delta G_2^*(0)^2\}^{1/2} \quad (5)$$

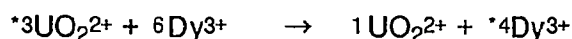
where  $\Delta G_2^*(0)$  is the intrinsic barrier to electron transfer, *i.e.* the activation free energy when  $\Delta G_2 = 0$ . Figure 2 shows a plot of  $k_q$  versus  $\Delta G_2$  for various N-heteroaromatic compounds using eq. (3). Although Fig. 2 shows some scatter, the calculated curve almost coincides with the experimental data. According to the Rehm-Weller correlation, the plot of  $\log k_q$  versus  $\Delta G_2$  is expected to give a linear line with a slope of  $-1/2.3RT$  ( $16.9 \text{ eV}^{-1}$ ) in the sufficiently endergonic  $\Delta G_2$  region. In the quenching of uranyl emission with various series of quenchers, the values of  $-\log k_q / \Delta G_2$  are reported to be much smaller ( $0.2- 2 \text{ eV}^{-1}$ ) than  $16.9 \text{ eV}^{-1}$ . In our study, the value of  $-\log k_q / \Delta G_2$  in N-heteroaromatic compounds is nearly equal to  $16.9 \text{ eV}^{-1}$  and this is a special case in uranyl photoreactions. These results can be reasonably explained by the large  $\pi$ -bonding ability of N-heteroaromatic compounds towards  $^*UO_2^{2+}$  yielding the formation of relatively stable exciplex (or an encounter complex), and  $\Delta G_2^*(0)$  is nearly equal to the value predicted by the Rehm-Weller correlation.

#### *Energy Transfer from the Excited Uranyl Ion to Dysprosium Ion*

In solutions containing  $UO_2^{2+}$  and  $Dy^{3+}$ , 414 nm laser irradiation resulted in the excitation of only  $UO_2^{2+}$ , because  $Dy^{3+}$  has no absorption at this wavelength. Under the above irradiation, the emission intensity  $I(t)$  at 570 nm showed a dual-exponential-function relation with time  $t$ :

$$I(t) = I(01)\exp(-t/\tau_1) + I(02)\exp(-t/\tau_2)$$

where  $I(01)$  and  $I(02)$  refer to the emission intensities at  $t = 0$  for two excited species and  $\tau_1$  and  $\tau_2$  are the lifetimes of these species. The  $t = 0$  is defined as the end of the irradiation pulse. The first term in the above equation can be assigned to the direct emission of excited uranyl ion  $^*UO_2^{2+}$  and the second term to the emission of excited dysprosium ion  $^*Dy^{3+}$  as mentioned below. The lifetime of term,  $\tau_2 = (2.5 - 3.0) \times 10^{-6}$  s, which is independent of the concentration of  $Dy^{3+}$ , agrees well with reported value for the lifetime of  $^*Dy^{3+}$ . In contrast, the lifetime of the first term,  $\tau_1$ , decreases with increasing concentration of dysprosium ion,  $[Dy^{3+}]$ , and this behavior correlates well with the quenching of uranyl emission. The rate constant for the quenching of  $^*UO_2^{2+}$  by  $Dy^{3+}$  was determined to be  $k_q = 2.01 \times 10^6 \text{ mol}^{-1} \text{ dm}^3 \text{ s}^{-1}$  from the Stern-Volmer plot. The sensitized emission of  $Dy^{3+}$  was not observed in fluorospectrophotometric measurements in  $D_2O$  solutions, but was observed in the differential spectrum at  $0.5 \mu\text{s}$  by the flash photolysis method. We also determined a decay constant at 578 nm from the time-resolved differential emission spectra which was in good agreement with the reported value for  $^*Dy^{3+}$ . These results clearly indicate that energy transfer takes place from the excited uranyl ion to the dysprosium ion. The sensitized process can be described by



#### *Laser Irradiation Nuclear Magnetic Resonance*

Laser Irradiation Nuclear Magnetic Resonance has been developed in our research group, which enable us to record high resolution NMR spectra under the irradiation of a laser. The  $^{17}O$  NMR spectra of uranyl oxygen atoms (oxygen atoms of  $UO_2^{2+}$ ) were measure by this method. The irradiation system is shown in Fig. 3, where a laser beam passes through the inside of temperature controller, which regulates the ample temperature, and irradiates an NMR sample from the bottom of sample tube with a flux 4 mm in diameter. By using this technique, the resolution of NMR spectra is kept unchanged during laser irradiation and the intensity of the irradiating laser is very stable. A JEOL JNM-FX 100 NMR spectrometer and a Spectra Physics Series 200 argon-ion laser were used. In our earlier papers, the  $^{17}O$  NMR spectra of uranyl oxygens were so narrow that three signals due to the

isotopomers, *i.e.* [ $^{16}\text{O-U-}^{17}\text{O}$ ], [ $^{17}\text{O-U-}^{17}\text{O}$ ], and [ $^{18}\text{O-U-}^{17}\text{O}$ ], were observed. Figure 4 shows the  $^{17}\text{O}$  NMR spectra of uranyl oxygens under the irradiation of a 488 nm laser as a function of output power (W), which is proportional to the laser intensity as calibrated by a radiometer. Two peaks were observed and assigned from the lower field as signals of [ $^{16}\text{O-U-}^{17}\text{O}$ ] and [ $^{18}\text{O-U-}^{17}\text{O}$ ], respectively. It can be seen in this figure that as output power, or laser intensity increased the signals shifted to the lower field, and their linewidths became broader, becoming a single peak at the high output powers. McGlynn and Smith reported that the long-lived excited state was triplet either  $^3\Pi_u$  or  $^3\Delta_u$  (with a preference for the former), and that the anisotropy of the paramagnetic susceptibility in the  $^3\Pi_u$  state was maximal parallel to the O-U-O axis. This is consistent with the above result that the paramagnetic result is remarkable in the axial oxygens and little effect is observed in equatorial water. Since  $^*\text{UO}_2^{2+}$  is in rapid equilibrium with  $\text{UO}_2^{2+}$  within the time scale of NMR measurements, *i.e.* the lifetime of  $^*\text{UO}_2^{2+}$  in acidic aqueous solutions is ca  $10^{-6}$  s $^{-1}$ , the observed paramagnetism in NMR spectra should be proportional to the concentration of  $^*\text{UO}_2^{2+}$ .

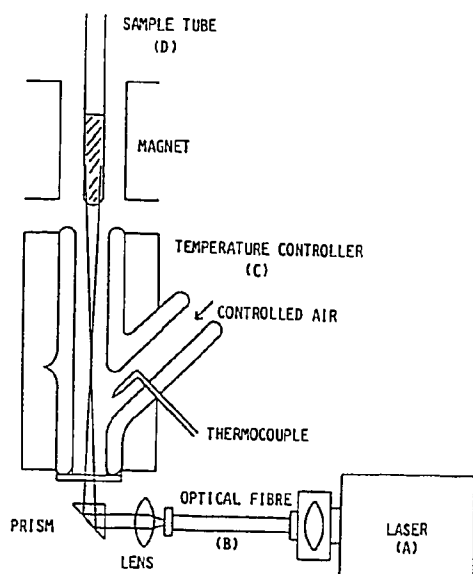


Fig. 3 Scheme of laser-irradiation system. The system consists of four main components: (A) laser, (B) optical fibre, (C) temperature controller and (D) sample tube.

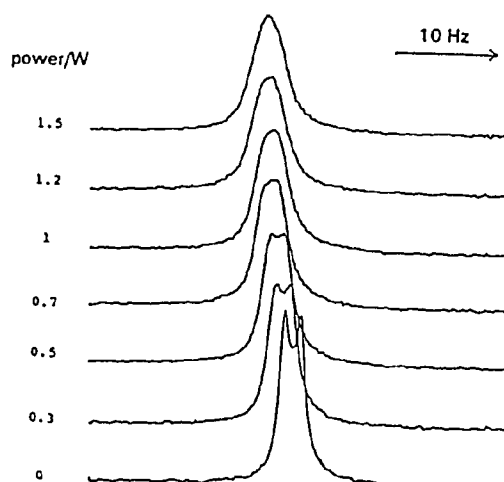


Fig. 4  $^{17}\text{O}$  NMR spectra of uranyl oxygens as a function of laser power (W).

### III Photo-reduction of Uranyl Ion

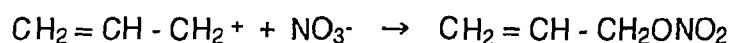
#### *Photo-reduction of the Uranyl Ion with Inorganic Compounds*

Photochemical reactions of the uranyl(VI) ion with halogen and halogen-like anions, I<sup>-</sup>, Br<sup>-</sup>, Cl<sup>-</sup> and NCS<sup>-</sup>, were investigated in aqueous phosphoric acid solutions under the irradiation of nitrogen laser. The formation of U(IV) was observed in the reactions with I<sup>-</sup>, Br<sup>-</sup>, and NCS<sup>-</sup>, but not with Cl<sup>-</sup>. The yield of U(IV) increases in the order, Br<sup>-</sup> < NCS<sup>-</sup> < I<sup>-</sup>. This order is the same as that of  $k_q(X^-)$  and the reverse of the standard potentials of these anions. The results are consistent with the electron transfer mechanism between excited uranyl ion and these halogen and halogen-like anions in the primary process. On the other hand, in the photo-reaction between U(IV) and Fe(phen)<sub>3</sub><sup>2+</sup>, since Fe(phen)<sub>3</sub><sup>2+</sup> has strong absorbance in the visible region, *i.e.* the molar extinction coefficient is larger than 10<sup>4</sup> mol<sup>-1</sup> dm<sup>3</sup>cm<sup>-1</sup> at 510 nm, the decreasing rate of Fe(phen)<sub>3</sub><sup>2+</sup> can be measured while holding the U(IV) concentration constant under the condition  $[U(VI)]_0 \gg [Fe(phen)_3^{2+}]_0$ , where  $[ ]_0$  denotes the initial concentration. Figure 5 shows plots of  $-\ln(A_t - A_f)$  versus  $t_{irr}$ , where  $A_t$  and  $A_f$  refer to the absorbances at  $t_{irr}$  and infinity, respectively, in the oxygen free and oxygen saturated solutions. In Fig. 5, the plot shows a curvature in the oxygen free solution, while is linear in the oxygen saturated solution. It was concluded clearly that the role of U(V) was important for this reaction, because the oxidation of U(V) by solvated oxygen changed the rate equation.

#### *Photo-reduction of the Uranyl Ion with Alkenes*

Photochemical reactions of U(VI) with alkenes, 1-heptene, 1-hexene, 1-octene, cycloheptene, cyclohexene; 1,4-cyclohexadiene, 2,4-hexadiene and 1,3-cyclohexadiene, were performed by irradiating with a high pressure mercury lamp through a filter cutting off wavelength shorter than 400 nm in perchloric acid solutions. It was found that the quantum yields for the formation of U(IV) was larger in alkene with smaller vertical ionization potentials. The formation of U(IV) was not observed in 1-heptene, 1-hexene and 1-octene, but U(IV) was produced if NaNO<sub>3</sub> was added to the same solutions. Because of  $\pi$ -bonding ability of alkenes, it is reasonable to presume that \*U(VI) interacts with an alkene to form an encounter complex or exciplex [<sup>\*</sup>UO<sub>2</sub><sup>2+</sup>...Q], which is subject to intramolecular electron transfer

from the alkene to  $^*U(VI)$  to form an unstable intermediate  $[UO_2^+ \dots Q^+]$  as described for the reaction between  $^*U(VI)$  and N-heteroaromatic compounds. The intermediate  $[UO_2^+ \dots Q^+]$  either decomposes to form  $UO_2^{2+}$  or proceeds to the  $k_3$  path; hence only  $k_4/(k_3 + k_4)$  contribute to the formation of U(V). The addition of nitrate to the solutions results in the formation of U(IV) even though nitrate is a good oxidizing reagent. It was reported that nitrate reacted with the propylene cation radical as



Based on the above reaction, since  $NO_3^-$  only slightly quenches  $^*UO_2^{2+}$ ,  $NO_3^-$  stabilizes  $UO_2^+$  by quenching  $[UO_2^+ \dots Q^+]$  and  $Q^+$ , and as a result the addition of  $NO_3^-$  would assist the formation of U(IV).

#### IV Photo-oxidation of Uranium (IV) and Plutonium(III) in Nitric Acid Solutions

Oxidation of U(IV) in nitric acid solutions was studied in dark and under the irradiation of Xenon light. Experiments were carried out in terms of the conventional spectrophotometric method. Figure 6 illustrates a pseudo first-order plot in dark, a plot of  $(A_t - A_f)$  versus time. As seen in Fig. 6, the plot is linear only in the initial stage and tends to curve resulting from the acceleration of reaction. This curvature is attributed to the additional reaction path of U(IV) with nitrous acid, which is formed by the reduction of nitrate. As a matter of fact, reaction became much faster, if  $HNO_2$  was previously added to the solution. It was found that the irradiation of light above 420 nm results in no gain for the apparent oxidation rate of U(IV). This obviously indicates that U(IV) is not sensitive for photo-reaction and that only excitation of  $NO_3^-$  should be taken account of.

The above reaction is basically similar to the photo-oxidation of plutonium(III) performed by Wada and coworkers. The purpose of this study is to separate plutonium from solutions containing neptunium by using photochemical reactions. Under the irradiation of Hg lamp, Pu(III) was selectively oxidized to Pu(IV) without changing Np(V).

#### Acknowledgement

The studies (Ref. 1-12) reviewed in this paper were performed in cooperation

with Dr. Yoon Yul Park of Pusan Junior College, Dr. Yasuhisa Ikeda of Institute of Research and Innovation, Mr. Yukio Wada of Power Reactor and Nuclear Fuel Development Co., and Masayuki Harada, Tomoo Yamamura and Koh Hatakeyama of author's colleagues in Tokyo Institute of Technology. The author wishes to thank them for their helpful cooperations.

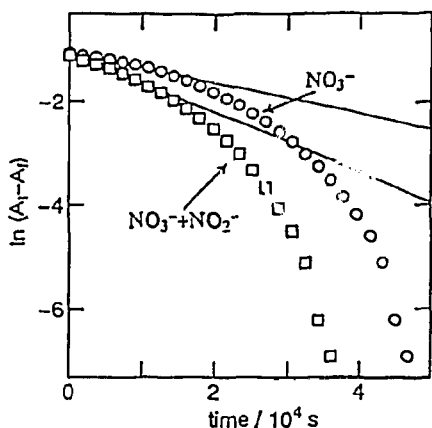


Fig. 6 Pseudo first order plot for the oxidation of U(IV) by  $\text{NO}_3^-$  in dark (O) and the same plot for the solution, in which  $\text{HNO}_2$  (0.03M) was previously added, (□) under the condition:  $[\text{U(IV)}] = 0.009 \text{ M}$ ,  $[\text{NaNO}_3] = 0.3 \text{ M}$ , and  $[\text{H}^+] = 0.5 \text{ M}$  at at ionic strength = 3.5 M and at 40 °C.

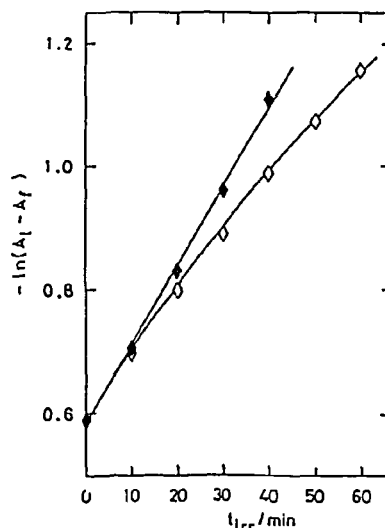


Fig. 5 Plots of  $-\ln(A_t - A_f)$  vs.  $t_{irr}$  in oxygen free (◇) and oxygen saturated (◆)  $2 \text{ mol} \cdot \text{dm}^{-3}$  phosphoric acid solutions at 25°C  
 $[\text{U(VI)}]_0 = 5.0 \times 10^{-2} \text{ mol} \cdot \text{dm}^{-3}$ ;  
 $[\text{Fe(phen)}_3^{3+}]_0 = 5.0 \times 10^{-3} \text{ mol} \cdot \text{dm}^{-3}$ .

## References

- 1) Park, Y.Y., Sakai, Y., Abe, R., Ishii T., Harada, M., Kojima, T., and Tomiyasu, H.: J. Chem. Soc., Faraday Trans., 86 (1990).
- 2) Yamaguchi, T., Harada, M., Park, Y.Y., and Tomiyasu, H.: J. Chem. Soc., Faraday Commun., 1621 (1990).
- 3) Harada, M., Sakamaki, S., Yamaguchi, T., and Tomiyasu, H.: Nihon Kagakukai Shi, 951 (1992).
- 4) Mizuguchi, K., Ikeda, Y., Harada, M., Park, Y.Y., and Tomiyasu, H.: J. Nucl. Sci. Technol., 30, 542 (1993).
- 5) Yamamura, T., Park, Y.Y., Tomiyasu, H.: J. Alloy Compounds, 193, 186 (1993).
- 6) Yamamura, T., Iwata, S., Iwamura, S., and Tomiyasu, H.: to be published .
- 7) Park, Y.Y., Harada, M., Ikeda, Y., and Tomiyasu, H.: J. Nucl. Sci. Technol., 28, 418 (1991)
- 8) Park, Y.Y. and Tomiyasu, H.: J.Photochem. Photobiol., 74, 11 (1993).
- 9) Park, Y.Y., Ikeda, Y., and Tomiyasu, H. RECOD'91, Sendai, Vol.II, 814 (1991).
- 10) Park, Y.Y. and Tomiyasu, H.: J.Photochem. Photobiol., 64, 25 (1992).
- 11) Hatakeyama, K., Park, Y.Y., Tomiyasu, H. Wada, Y., and Ikeda, Y.: Global-93, Seattle, 1325 (1993).
- 12) Wada, Y., Goibuchi, T., Morimoto, K., and Tomiyasu, H.: Actinide-93, Santa Fe, 14 (1993).
- 13) Wada, Y., Wada, K., Goibuchi, T., and Tomiyasu, H.: J. Nucl. Sci. Technol (1994), in press.